

Tools for Quantitative and Validated Measurements of Cells

Anne L. Plant, John T. Elliott, Alessandro Tona, Dennis McDaniel,
and Kurt J. Langenbach

Summary

In this chapter, we describe the preparation of thin films of collagen that can serve as reference materials for assuring reproducible and predictable cell responses. Subtle differences in the molecular-scale characteristics of extracellular matrix proteins, including the supramolecular structure of type 1 collagen, can have tremendous influences on cell state and cell-signaling pathways; therefore the careful control and analysis of the culture surface is critical to assure a relevant and consistent response in cell-based assays. We also describe how cell-phenotypic parameters such as morphology, proliferation, and green fluorescent protein expression can be unambiguously quantified in adherent cells by automated fluorescence microscopy or high content screening. Careful consideration of protocols, and the use of fluorescent reference materials, are essential to assure day-to-day and instrument-to-instrument interoperability. The ability to collect quantitative data on large numbers of cells in homogeneous matrix environments allows assessment of the range of phenotypes that are reproducibly expressed in clonal cell populations. The inherent distribution of responses in a cell population will determine how many cells must be measured to reach an accurate determination of cellular response.

Key Words: Alkanethiol self-assembled monolayers; automated fluorescence microscopy; extracellular matrix protein; green fluorescent protein; type 1 collagen.

1. Introduction

The National Institute of Standards and Technology (NIST) is considered the nation's measurement institute. With more than a 100 yr history, NIST technology, measurements, and standards are geared to help US industry invent and manufacture superior products reliably, provide critical services, ensure a fair marketplace for consumers and businesses, and promote acceptance of US products in foreign markets. As industrial and national priorities have evolved, NIST has responded by expanding its portfolio into new strategical directions, such as biotechnology. The physical measurement capabilities and approaches that NIST is best known for are now routinely being applied to biological molecules such as DNA and proteins, and more recently, to cells (e.g., see http://www.cstl.nist.gov/biotech/Cell&TissueMeasurements/Main_Page.htm).

A major challenge facing the biotechnology and pharmaceutical industries today is the ability to quantitatively assess biomarker expression in living cells. Drug screening and toxicology relies increasingly on cell-based assays, with the hope that quantitative cell response will provide a more reliable predictor of clinical outcome than molecular-scale screening

approaches. High content screening has permitted a high throughput approach to fluorescence-based imaging (see Chapter 1). However, the validity, reproducibility, interoperability, and interpretation of such data are currently less than perfect. Establishing an *in vitro* model system that accurately reflects *in vivo* response will likely remain a challenge for years to come. However, the development of improved matrices and quantitative methodologies will help the community make more reliable, reproducible, interoperable, and meaningful cell-based measurements.

Our group is developing cell metrology tools that will help minimize sources of variability in conducting quantitative cell biology measurements and facilitate interlaboratory data comparability. The components of this toolkit include thin films of extracellular matrix (ECM) proteins, which are highly reproducible and amenable to analysis by independent methods, and quantitative fluorescence microscopy protocols that allow accurate and reproducible quantification of cell response; these tools are discussed in this chapter. We are also developing lines of indicator cells that allow nearly real time, *in situ*, evaluation of growth conditions such as growth matrices, serum, and pharmaceuticals. These tools will facilitate applications such as diagnostic assays, drug screening, pharmaceutical development, development of biomaterials, and determination of culture conditions for stem cells. In addition, such reference materials and protocols will be essential for standardizing and validating data on cells and tissues that might be compiled into databases for use in modeling complex biological networks.

1.1. Thin Films of Collagen as Reference ECM

ECM proteins can induce diverse intracellular signals by providing both mechanical and chemical stimuli to cells (1). Owing to signal pathway crosstalk, these intracellular signals will mitigate and be affected by other sources of cell signals. Because of the importance of ECM cues in poising cell-signaling pathways, careful control of the ECM might be extremely important when studying cellular response to soluble factors such as pharmaceuticals. In addition, well-defined matrices provide the opportunity to understand the role of the matrix cues in cell response, which is difficult with serum protein-coated tissue culture polystyrene in which the identity and presentation of matrix molecules are difficult to know.

Collagen is the major structural protein in tissues. We have developed a reliable method for fabricating reproducible thin films of native type-1 and denatured type 1 collagen (2). Thin films of native collagen are determined by ellipsometry measurements to range from about 6 to 40 nm thick depending on the concentration of collagen in the solution from which they are assembled. The thin films are formed by allowing collagen in solution to self assemble onto gold-supported alkanethiol monolayers as depicted in Fig. 1. As shown in Fig. 1, at low concentrations of collagen in solution, the surface is primarily covered by a layer of very small collagen fibrils; and large fibrils grow out of the small fibrils (Fig. 1C). These large fibrils are about 200 nm in diameter, can be microns in length, and appear to be pinned at one end to small fibrils at the surface. A thin film made up of exclusively of short fibrils appears to present different mechanical signals to cells than do thin films containing large fibrils. This will be discussed in greater detail later.

Vascular smooth muscle cells (vSMC) and fibroblasts response to thin films of large collagen fibrils is analogous to their response to collagen gels with respect to cell morphology, proliferation rate, cytoskeleton organization, expression of the tenascin-C gene, ERK1/2 phosphorylation, and $\alpha_2\beta_1$ integrin engagement (3,4). Unlike collagen gels, the thin films are rugged, highly reproducible, and homogeneous. Furthermore, they are optically superior to collagen gels because they scatter less light, and because they are homogeneous in thickness, cells in different fields are in approximately the same focal plane. These characteristics make them amenable to automated microscopy. These thin films provide a matrix environment that is identical from

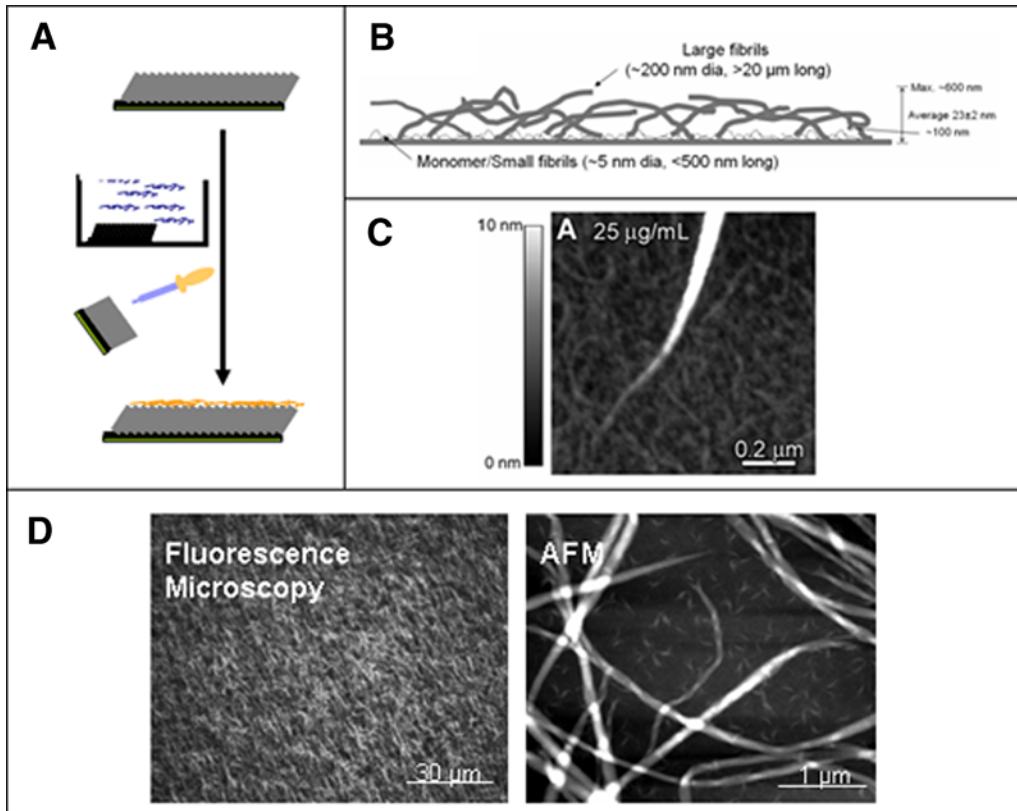


Fig. 1. Thin films of type 1 collagen. (A) Hydrophobic alkanethiol monolayers are self-assembled on translucent layers of gold on glass slides. Thin films of collagen are formed by placing the alkanethiol-coated slide into a solution of monomeric type 1 collagen at neutral pH and physiological ionic strength. After overnight at 37°C, the surfaces are rinsed, dried briefly under a stream of N₂, and replaced into buffer or medium. (B) Ellipsometry measurements indicate that thin films prepared from 300 µg/mL collagen solutions have an apparent thickness of approx 23 nm according to an effective medium model. (C) Atomic force microscopy of collagen films prepared from a low concentration of collagen shows that a layer of very small fibrils underlay larger fibrils and that larger fibrils appear to be connected to, and grow out of, the smaller fibrils. The dimensions of the small fibrils are consistent with an aggregate of five collagen triple-helix monomers. (D) Atomic force microscopy (right) indicates that the large fibrils are on the order of 200 nm in diameter and tens of microns long. Fluorescence microscopy of fluorophore-labeled collagen thin films (left) indicates that the films are spatially homogeneous.

field-to-field and from experiment-to-experiment, and cells display a predictable and highly reproducible response on these films. Because these films can be characterized by a variety of surface analytical techniques such as ellipsometry, surface plasmon resonance, and scanning probe microscopies, one can verify the homogeneity and reproducibility of the cell culture surface independently from the cell response.

Thin films of collagen are excellent substrates for observing cell structure and cell-matrix interactions by light microscopy techniques. The thin film approach also allows us to systematically modify the ECM environment to observe that subtle differences in ECM protein conformation and supramolecular structure can alter cell response. For example, the surface free energy of the substrate onto which type 1 collagen adsorbs determines the supramolecular structure of

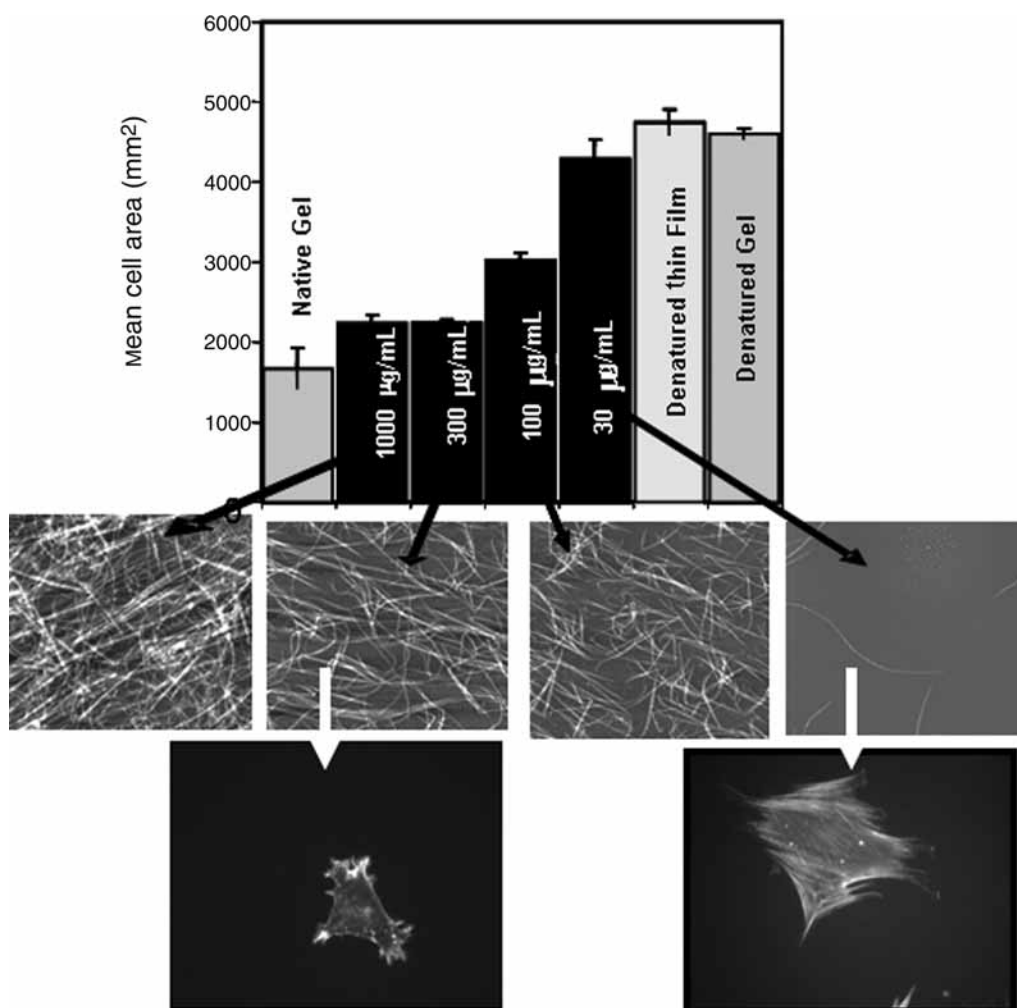


Fig. 2. Evidence for mechanical influence on cellular response. Thin films of collagen on alkanethiol monolayers prepared from higher concentrations of collagen in solution have a denser film of large collagen fibrils, and thin films prepared from low concentrations of collagen consist primarily of the very small fibrils of collagen that are in very close proximity to the alkanethiol monolayer. The cells that interact with large fibrils (left) do not spread significantly, and have a poorly organized cytoskeleton compared to the cells that interact primarily with small collagen fibrils, which are much more spread (left) and have well-organized stress fibers as seen by staining with phalloidin. Cells on the surfaces prepared from low concentrations of collagen also are more proliferative and demonstrate changes in gene expression compared to the cells on the more physiologically relevant collagen on the left. Other experiments have shown that cells interact with both surfaces identically through the β_1 -integrin receptor.

adsorbed collagen. On hydrophilic surfaces such as glass, collagen adsorbs as a monomer, but on more hydrophobic surface collagen forms fibrillar structures (5). Cells respond very differently to monomeric collagen than to collagen fibrils. We have also demonstrated that on hydrophobic surfaces exposed to different concentrations of collagen in solution, thin films will result that have different densities of large collagen fibrils. The density of large fibrils has a remarkable effect on cell morphology, proliferation, and gene expression, even in the absence of any changes in chemistry or integrin recognition. **Figure 2** shows the obvious differences in the

density of large collagen fibrils that form at alkanethiol surfaces as a function of differences in concentration of collagen in solution. These differences in collagen fibril density result in obvious differences in vSMC morphology and cytoskeletal organization. Further analysis has determined that the cells engage the same integrins on these surfaces, yet show distinct differences in gene expression and proliferation rate, in addition to differences in morphology. Ongoing work suggests that cells are responding to differences in the mechanical properties of large and small collagen fibrils.

1.2. Quantitative and Automated Microscopy

Quantitative measurements are essential for determining the results of a cell-based assay, and for verifying interoperability of cell-assay data collected on different days and in different laboratories (*see Note 1*). By making quantitative measurements, one can also assess the effect that time in culture or cryopreservation has on cell phenotype. Ultimately, quantitative interoperable data will be required for the development of the extensive cell-based bio-informatics databases and models that will make possible the understanding of signaling networks.

Figure 3 shows the novel use of Texas Red maleimide to provide a bright fluorescent stain to discern cell areas from noncell areas, which allows rapid cell identification, counting of cells, and morphology analysis on a cell-by-cell basis over large numbers of cells using automated microscopy (**6**). The use of a nuclear stain allows discrimination of Texas-Red-labeled objects that are not cells, and determination of how many cells are present as a cluster (**2**). The bright cell area defined by Texas Red staining can also be used as a “mask” for quantifying intracellular green fluorescent protein (GFP) and other intracellular fluorescent indicators. Robust protocols for quantitative automated fluorescence microscopy and imaging analysis facilitate measurements of statistically relevant numbers of cells in an unbiased fashion (*see Note 2*). Thin films of ECM aid automated microscopy because the optical properties of the substrate are homogeneous across the x - y plane. Thin films also tend to have reduced background scattering, making discrimination between cells and background greater. By automatically moving the stage to select fields, the experimenter is not responsible for locating “good” fields of cells. Many fields can be sampled, allowing for accumulation of data on large numbers of cells. By collecting data on a sufficient number of individual cells, the inherent variability of response within the population can be discerned.

1.3. Natural Variability Within Cell Populations

Even clonal populations of cells cultured on spatially homogeneous self-assembled matrices show a range of phenotypic responses. We have quantified the reproducible distributions of cell size, GFP expression, and phalloidin staining of filamentous actin in vSMC in contact with collagen films. This variability in response within the population is highly reproducible. **Figure 4** shows that vSMCs are less spread (*i.e.*, assume a smaller area) on thin films of collagen with a large density of collagen fibrils, compared to vSMC on tissue culture polystyrene. Although the average areas for cells on the two surfaces are distinctly different, on each surface there is a range of cell areas. It is clear that there is overlap in the amount of spreading of cells on the two different matrices, *i.e.*, for cells of intermediate size it cannot be distinguished based on the extent of spreading which surface they are growing on. Most cellular phenotypes will appear as a range of responses, even if the cell population arises from a single clone and the cells are all in a spatially homogeneous environment such as provided by a thin film of collagen fibrils. The average response is not necessarily an adequate representation of the cellular response especially when the distribution of responses is broad or non Gaussian. Analysis of the cumulative distributions provides a sensitive statistical treatment of the differences between distributions

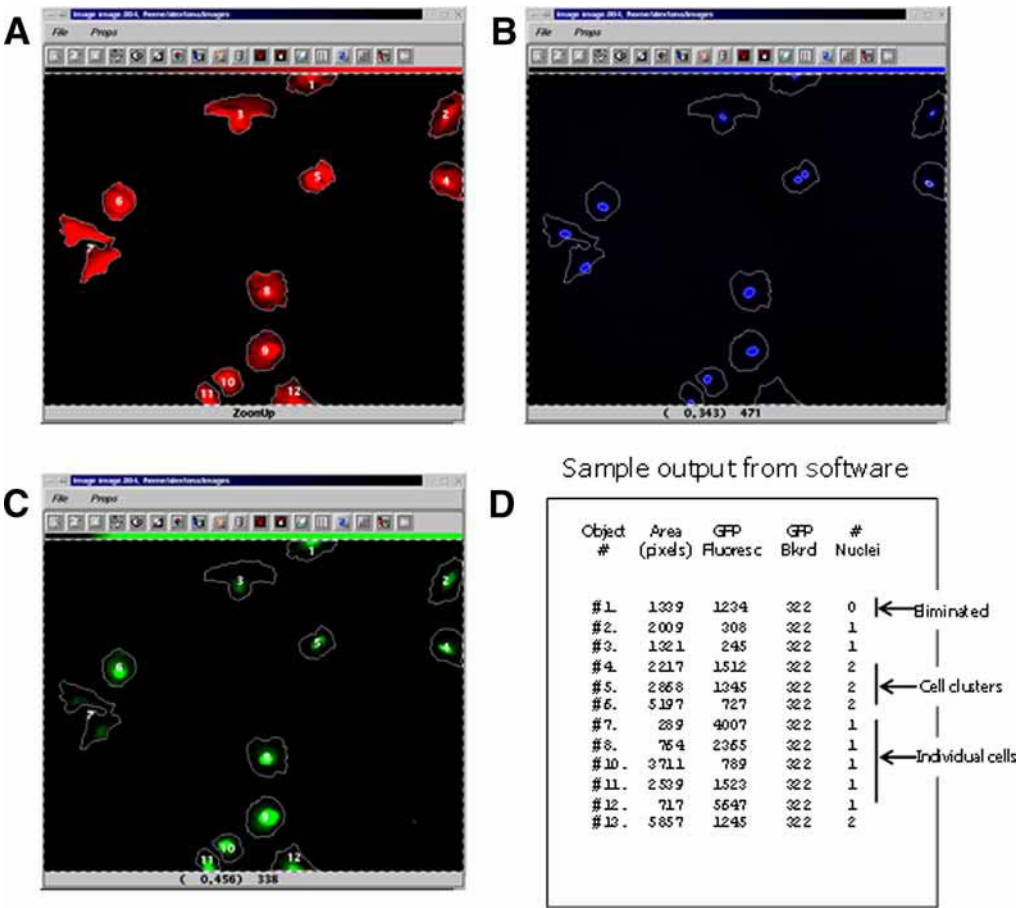


Fig. 3. Automated quantitative microscopy. (A) Staining with Texas Red maleimide allows good discrimination of cell edges from noncell background. The user sets a threshold pixel intensity value above which the pixel is recognized as part of an object. Each object is automatically detected and numbered. (B) Using another filter set, DAPI staining of cell nuclei is detected, allowing Texas Red-stained objects to be verified as cells or clusters of cells. (C) Using a third filter set, GFP inside of cells is detected allowing integration of the intensity of the pixels lying within the area identified by each cell object “mask” delineated in (A). (D) The presence or absence of nuclei in each object, the number of nuclei, the cell area (as determined from the number of Texas Red pixels per object), the integrated intensity of GFP (or other fluorophore) within the object mask, and the background fluorescence are automatically determined by the software routine along with other parameters.

(7,8). Quantifying and analyzing the statistics associated with the range of responses within the population also allows calculation of how many cells must be examined in order to achieve an accurate sampling of the population.

The collection of data from large numbers of cells (hundreds to thousands) provides the statistical assurance of the reproducibility of the observations. Although flow cytometry also allows collection of data on large numbers of cells, it does not permit examining cells adhered to matrix, eliminating the collection of data regarding cell morphology, and it does not provide the possibility of quantifying changes in cell response in real time. High content screening now allows these measurements in a high-throughput way, whereas human-interactive; imaging microscopy is still a valuable tool for lower throughput studies.

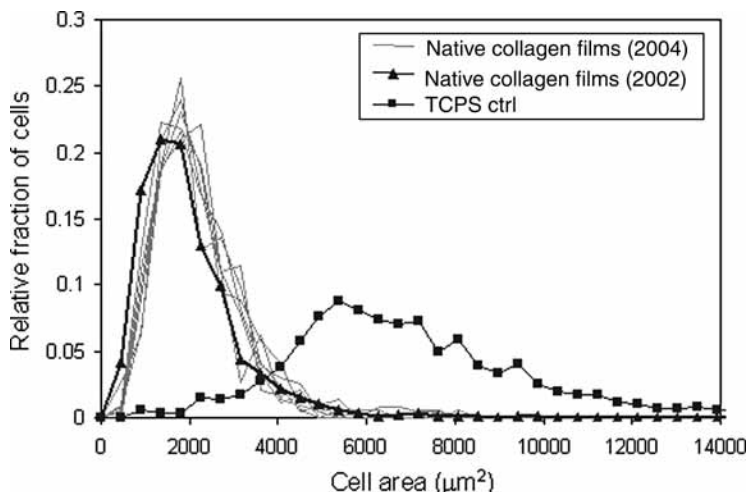


Fig. 4. Quantifying distributions of cellular responses. vSMCs (A10) respond to different kinds of collagen thin films in a large number of ways, including morphology. Cells on thin films of collagen with a high density of large collagen fibrils are minimally spread and assume a stellate morphology (gray lines). These cells spread to an average area of $2100 \mu\text{m}^2$. The cells on fibrillar collagen are significantly less spread than the same cells cultured on tissue culture polystyrene (black, square). These averages, and the range of the size observed, are highly reproducible and consistent from experiment to experiment. For example, morphology distributions of A10 cells cultured on the same day on replicate thin films of fibrillar collagen are nearly identical (gray lines). These distributions are plotted with the A10 morphology distribution collected from thin films of fibrillar collagen prepared by identical methods collected 12 mo earlier (black, diamond).

2. Materials*

2.1. Preparation of Alkanethiol-Coated Supports and Thin Films of Collagen

1. Sodium dodecyl sulfate (Bio-Rad, Hercules, CA).
2. H_2SO_4 (Mallinckrodt Baker, Paris, KY).
3. Potassium persulfate (Sigma, St. Louis, MO).
4. Deionized H_2O , purified through a Milli-Q Academic system (Millipore Corp, Bedford, MA).
5. Particle-free polyester cloth (Texwipe TX1010, Fisher Scientific, Springfield, NJ).
6. Polished Si wafers (Silicon, Inc. Boise, ID).
7. Kimwipes (Kimberly-Clark, Roswell, GA).
8. 1-Hexadecanethiol (Aldrich, Milwaukee, WI), used as 0.5 mM solution in absolute ethanol.
9. Teflon squirt bottles (Nalgene Nunc, Rochester, NY).
10. Vitrogen, a sterile solution of purified, pepsin-solubilized bovine dermal collagen dissolved in 0.012 N HCl (Cohesion Technologies, Palo Alto, CA).
11. 10X Dulbecco's phosphate-buffered saline (DPBS, Gibco Invitrogen, Carlsbad, CA; when diluted to 1X concentration, contains: 0.1 g/L CaCl_2 , 0.2 g/L KCl, 0.2 g/L KH_2PO_4 , 0.1 g/L $\text{MgCl}_2 \cdot 6\text{H}_2\text{O}$, 8 g/L NaCl, and 2.16 g/L $\text{Na}_2\text{HPO}_4 \cdot 7\text{H}_2\text{O}$).
12. 0.1 M NaOH (Sigma), sterilized by passing through 0.2-μm filter.

2.2. Cell Culture

1. DPBS, Ca^{2+} and Mg^{2+} free (Gibco Invitrogen).
2. Trypsin-EDTA solution (Sigma).

* Indication of specific manufacturers and products is for clarity only and does not constitute endorsement by NIST.

3. Rat aortic vSMC line, A10 (ATCC, Manassas, VA).
4. Dulbecco's modified Eagle's medium (DMEM; Mediatech, Herndon, VA).
5. L-Glutamine, 100X (Gibco Invitrogen).
6. MEM nonessential aminoacid solution, 100X (Gibco Invitrogen).
7. Penicillin-streptomycin solution, 100X, (Gibco Invitrogen).
8. Fetal bovine serum (FBS; Gibco Invitrogen).
9. 8-well polystyrene plates (Nalgene Nunc).
10. Mouse embryonic fibroblast cells (NIH3T3; ATCC).
11. 25 cm², vented cap tissue culture flasks, for routine culture (Corning, Corning, NY).

2.3. Cell Fixation, Staining, and Fluorescence Microscopy

1. Hanks Balanced Salt Solution (HBSS; ICN Biomedicals, Costa Mesa, CA).
2. DPBS, without CaCl₂ (Sigma).
3. Texas Red-C₂-Maleimide (Molecular Probes Invitrogen).
4. Bovine Serum Albumin, (BSA, Fraction V; Sigma).
5. Triton X-100 (Sigma).
6. Glycerol (Research Organics, Cleveland, OH).
7. 16% Paraformaldehyde (Electron Microscopy Sciences, Hatfield, PA).
8. Ammonium chloride (Sigma).
9. 1,4-Diazabicyclo(2,2,2)octane (DABCO, Sigma).
10. 4',6-Diamidino-2-phenylindole (DAPI, Sigma).
11. No. 1 coverglass slides (Nunc, Naperville, IL).
12. Fluorescein-isothiocyanate-phalloidin (Sigma).
13. 3-Maleimido-benzoic acid-NHS ester (MBS), Sigma.
14. DMF (dimethylformamide, Sigma).
15. Microtubule stabilizing buffer (MTSB): 100 mM PIPES (piperazine-*N,N'*-bis[2-ethanesulfonic acid, Sigma), 1 mM ethylene glycol-bis(2-aminoethyl)-*N,N,N',N'*-tetraacetic acid (Fluka, Milwaukee, WI), 4% polyethylene glycol 8000 (Fluka), adjusted to pH 6.9.
16. Long Pass GG475 (Schott) Glass Filters (Edmund Optics, Barrington, NJ).
17. NIST SRM 1932 fluorescein solution (NIST, Gaithersburg, MD).
18. Optical filters: emission filters, D460/50, HQ525/50, S630/60, No. 84101 (multi bandpass); excitation filters, D360/40, HQ470/40, S555/25; Beam Splitters, BS No. 51019 (triple bandpass), No. 84100 (quadruple bandpass); (Chroma Technologies, Brattleboro VT).

3. Methods

3.1. Preparation of Alkanethiol-Coated Supports

1. Glass cover slips (No. 1, 22 × 22 mm²) were washed in 1% (w/v) sodium dodecyl sulfate/water, rinsed extensively with deionized H₂O, and acid washed in fresh H₂SO₄ containing 10% potassium persulfate (30 min). The cover slips were rinsed extensively with deionized H₂O, transferred to acetone and dried on a particle free polyester cloth.
2. Polished Si wafers were cleaned by wiping them across an ethanol soaked Kimwipe and then a dry Kimwipe. Residual fiber and dust particles were removed under a stream of particle-filtered N₂.
3. Cover slips and wafers were coated with a layer of chromium (approx 1 nm) and a layer of gold (approx 7 nm) by magnetron sputtering using an Edwards (Wilmington, MA) 306 vacuum system equipped with two (approx 10 cm diameter) magnetron sputtering sources (one for chromium, the other for gold). The base vacuum level is typically better than 2 × 10⁻⁵ Pa (2 × 10⁻⁷ mbar). The argon pressure, 0.1 Pa (6 × 10⁻³ mbar), is kept constant during the sputtering process using an MKS Instruments (Andover, MA) Baratron butterfly valve. During sputtering the sample holder and samples are rotated over the gold and chromium targets (purity 99.99%) using a Superior Electric (Bristol, CT) SLO-SYN stepper motor system. A specially shaped mask is placed between the targets and the sample holder to ensure uniformity of film thickness over the whole sample surface. A DC power source applies 750 W for gold and 440 W for the chromium depositions. The substrate rotation time required to produce a given film thickness was determined with the help of X-ray and neutron reflectivity measurements on test samples. Atomic force

microscopy measurements on freshly prepared samples indicated that the gold surface roughness was <1 nm rms (measured over $25\ \mu\text{m}^2$).

4. The gold-coated wafers and cover slips were immersed in 1-hexadecanethiol (0.5 mM; Aldrich) in ethanol for at least 8 h before being rinsed with ethanol and dried with filtered N_2 . Alkanethiol-coated samples could be stored under ethanol for at least 7 d without any loss in performance.

3.2. Preparation of Thin Films of Type 1 Collagen

1. To prepare thin films of native collagen, translucent alkanethiol-treated gold-coated cover slips or Si wafer pieces were placed into neutralized solutions of native type 1 collagen monomer in DPBS (4°C).
2. To prepare the neutralized collagen solution, the cold solution of Vitrogen (acid extracted collagen monomer) was mixed with cold concentrated (10X) DPBS, and then with cold 0.1 M NaOH in a ratio of 8/1/1 (v/v/v) to achieve physiological pH and ionic strength conditions under which collagen monomer readily polymerizes into fibrils at 37°C .
3. The cover slips were immersed in 3 mL of collagen solution in eight-well polystyrene plates and were then incubated overnight at 37°C to allow polymerization of the collagen.
4. The collagen-coated samples were removed, rinsed with a stream of DPBS, and then deionized water from sterile Teflon squirt bottles (Nalgene Nunc).
5. Once all loosely adhered gel was removed, the samples were dried briefly (for approx 30–60 s) under a stream of filtered N_2 and immediately placed back into a DPBS solution (*see Note 3*). The samples were stored in DPBS at 4°C until they were used.

3.3. Characterization of Thin Films of Type 1 Collagen

1. The thickness of the collagen thin films on Si was determined by spectroscopic ellipsometry (J. A. Woollam, Lincoln, NE, Model M-44) in air using a two-layer model. The optical constants of the first layer were determined empirically from ellipsometric data collected for a control sample of alkanethiol-treated, gold-coated Si wafer. The optical constants of the second layer were fixed to $n = 1.45$ and $k = 0$ to approximate the properties of the protein film and the average thickness of the second layer for each sample was determined using the manufacturer's fitting routine.
2. The collagen samples were imaged using an atomic force microscopy with a magnetically driven Si tip in intermittent contact mode (PicoScan; Molecular Imaging, Phoenix, AZ). The thin films of collagen were imaged in air before they were placed into the fluid cell and imaged under DPBS. The results indicated that rehydrated and dry samples were qualitatively the same topographically. Images were taken from several areas on each sample to ensure the homogeneity of surface features. Images were flattened and, in some cases, plane fitted with the PicoScan software to improve visualization, and analysis of the images.

3.4. Cell Culture and Preparation of Cells for Experiments

1. The rat aortic vSMC line, A10, was maintained in DMEM supplemented with nonessential amino acids, glutamine, penicillin (100 U/mL), streptomycin (100 $\mu\text{g}/\text{mL}$), and 10% (v/v) FBS, and maintained in a humidified 5% (v/v) CO_2 balanced-air atmosphere at 37°C .
2. Subconfluent cultures were switched to supplemented DMEM containing 2% (v/v) FBS 24 h before an experiment. The reduced serum concentration maximizes the extent of cell signaling that is because of the ECM and mimics conditions that have been typically used in characterizing the response of these cells to native and denatured collagen gels (9).
3. Cells were removed from tissue culture polystyrene flasks by trypsinization, washed with DMEM/2% FBS and plated in DMEM/2% FBS onto the collagen substrates at a density of 2000 cells/ cm^2 except where indicated. The cell density was chosen to maximize the number of individual (nonclustered) cells on the substrate. Care was taken to ensure the seeding density was homogeneous over the surface of the substrates.
4. Cells were typically incubated at 37°C for 24 h except in the proliferation and integrin blocking experiments. All experimental incubations were performed with the thin films of collagen on gold-coated glass cover slips on the bottom of eight-well polystyrene plates.

3.5. Cell Fixation and Staining for Morphology Analysis

1. After incubation, samples were left in the wells of the polystyrene plates and the adhered cells were washed with warm HBSS, fixed in 4% (v/v) formaldehyde in DPBS (30 min) at room temperature, quenched in 0.25% (m/v) NH_4Cl in DPBS (15 min), and rinsed with DPBS.
2. Cells were permeabilized and stained (1 h) with Texas Red- C_2 -maleimide (10 mg/mL in dimethylformamide stock, dissolved in DPBS (0.5 $\mu\text{g}/\text{mL}$) containing 0.1% (v/v) Triton X-100.
3. Cells were rinsed once with DPBS, DPBS containing 1% (m/v) BSA and DPBS. DPBS-glycerol (1/1 v/v) containing 0.25% (m/v) 1,4-DABCO to reduce photobleaching, and 1.5 $\mu\text{g}/\text{mL}$ DAPI as a nuclear counterstain, was added to each well.
4. Samples were removed from the polystyrene wells and were placed upside down onto a drop of Tris-buffered saline (10 mM Tris, 140 mM NaCl, pH 8.5) containing 90% (v/v) glycerol, 0.25% DABCO and 1.5 $\mu\text{g}/\text{mL}$ DAPI on No. 1 glass slides.
5. The samples were clamped to the slides with small alligator clips, rinsed extensively with distilled water, dried under a stream of air and sealed at the edges with nail polish. This procedure significantly reduces the optical artifacts because of the presence of excess glycerol or dried buffer salts on the cover slips. Throughout the fixation and staining procedure, cell samples were always kept immersed in solution.
6. For filamentous actin staining, cells were permeabilized with 0.1% (v/v) Triton X-100 in DPBS (5 min), rinsed with DPBS, blocked with DPBS containing 3% (m/v) BSA blocking solution (30 min), stained with fluorescein-isothiocyanate-phalloidin in blocking solution (200 nM, 1 h), and rinsed with blocking solution.
7. The phalloidin-stained samples were rinsed extensively with DPBS and mounted on slides in Tris buffered saline containing 90% (v/v) glycerol, 0.25% (m/v) DABCO and 0.05 $\mu\text{g}/\text{mL}$ DAPI.
8. Cells were imaged with phase and fluorescence microscopy using the appropriate filter sets.

3.6. Cell Fixation and Staining for Quantifying Cellular GFP

1. Samples were removed from the incubator after 8 h, adhered cells were rinsed with warm HBSS supplemented with 10 mM HEPES and fixed for 24 h at room temperature in MTSB containing 100 $\mu\text{g}/\text{mL}$ MBS as the crosslinker (10) (see Note 4).
2. Cells were permeabilized in 0.05% Triton X-100 in DPBS for 5 min, rinsed in DPBS, and incubated with DPBS containing Texas Red- C_2 -maleimide (1 ng/mL) as a general cell membrane stain and 0.05% DAPI as a nuclear counter stain.
3. After 2 h at RT, 1% BSA was added to quench the conjugation reaction and the samples were rinsed with DPBS.
4. The samples were mounted onto No. 1 glass slides with 9/1 glycerol/Tris (v:v), pH 8.0 and the cells were imaged with fluorescence microscopy in an automated mode.

3.7. Automated Microscopy for Quantitative Analysis

1. The fixed and stained cells were examined by phase contrast and fluorescence microscopy using a 10X objective on an inverted microscope (Zeiss Axiovert S100TV, Thornwood, NJ) with a 100 W mercury arc lamp for fluorescence excitation, a computer controlled stage (LEP, Hawthorne, NY), an excitation and an emission filter wheel (LEP, Hawthorne, NY), and a CCD camera (CoolSnap fx, Roper Scientific Photometrics, Tucson, AZ). Hardware operation, and image digitization and analysis were under software control (ISee Imaging, Cary, NC).
2. A modular software routine controlled automated movement of the stage, autofocusing, and collection of data from 50 to 100 independent fields ($870 \times 690 \mu\text{m}^2$) of cells per sample. Autofocusing was performed on the Texas Red fluorescence of stained cells.
3. At each field cellular fluorescence from Texas Red, and then DAPI, was collected by automated switching of the appropriate excitation filters (S555/25 and D360/40, respectively) and passing the emitted light through a multipass beam splitter (No. 84100) and filter (No. 84101).
4. For measurements of GFP expressing cells, the multipass beamsplitter No. 51019 was used along with appropriate excitation and emission filters (D360/40 and D460/50 for DAPI, HQ470/40 and HQ525/50

for GFP, and S555/25 and S630/60 for Texas Red, respectively) (*see Note 5*). The excitation lamp intensity was checked every day using a 61 μM fluorescein solution (NIST SRM 1932) to allow for normalization of intensities with other data from other days.

5. Flat field correction was performed on all images. The flat fields were generated with a 475 nm long pass glass filter that exhibited broad fluorescence excitation and emission (*11*), which was placed on a No. 1 glass slide on the stage.
6. Appropriate thresholding of image data allowed cell areas, as determined by cellular Texas Red fluorescence, to be accurately distinguished from the nonfluorescent-noncell areas (*see Notes 6 and 7*).
7. For quantitative analysis of intracellular fluorescence such as GFP, the areas of Texas Red fluorescence that were associated with cells served as a “mask” to delineate the pixels associated with cells in identical fields of images collected with other filter sets. In this way, even cells that were not producing much GFP could be quantified even though their low GFP fluorescence might have otherwise precluded observing them.
8. Non-GFP fluorescence background was determined by eroding the area of the cell (i.e., including pixels immediately beyond the area of the cell), and using adjacent but noncell pixels to define the background intensity (*see Note 8*). The number of nuclei, and therefore the number of cells, was determined from the corresponding images collected with the DAPI filter. The requirement for spatial correspondence of DAPI and Texas Red fluorescence ensures that only cell areas with nuclei are used during data analysis.
9. Each cell area, cell roundness, and intracellular GFP intensity, as well as the number of nuclei in each field, were determined with image analysis software (ISee Imaging) as previously described (*2,6*). Data used to determine these parameters were collected from at least 200 cells on each sample.

4. Notes

1. *Intensity reference materials*: for standardizing fluorescence intensity measurements, a variety of reference materials can be used for checking lamp output. Fluorescent glass, solutions of high concentration of fluorophore, and fluorescent beads, for example, can all be used. Some materials prepared especially for this purpose can be purchased commercially. We have found that inexpensive semiconductor long pass glass filters that exhibit broad fluorescence excitation and emission have been useful for this purpose. (The glass filters in this series are fluorescent in different wavelength regions; coincidentally, 1 s integration times of GG475 at the wavelength regions of interest for DAPI, GFP, and Texas Red produced similar intensities.) The requirements for such a reference material include sufficient photostability, batch or solution reproducibility, appropriate intensity at desired wavelengths, and a linear fluorescence response to incident light. The use of this simple kind of intensity reference is only useful for providing relative information about the light source, and to verify that the instrument is functioning consistently; determining the transfer function for the collection optics is much more challenging.
2. *Image analysis software*: image analysis software packages are available from commercial and open source suppliers. One open source package is ImageJ, which is written in JAVA for platform-independent applications. Although any image analysis software package will have built in segmentation and data extraction techniques, it is likely that at least some algorithm development or testing will be required for particular applications. Development of robust algorithms for choosing appropriate threshold values or for reliable edge detection of cellular objects is still a challenge to be overcome. On our NIST web page we currently provide a set of image data for NIH3T3 cells that express GFP. The image set contains three fluorophores (Texas Red, DAPI, and GFP), and is provided for comparing edge detection and GFP quantification algorithms. With contributions from others in the community, we hope to add additional image sets from assays or staining procedures to create a comprehensive set of standard images to test algorithms development.
3. *Preparation of thin collagen films*: the volume, as well as the concentration of collagen monomer solution from which the thin films are made can effect the resulting structure of the collagen thin films. Brief drying with a stream of nitrogen or air after rinsing the thin films of collagen is required. If the films are not dried at all, many cells will remain round and die, possibly because the fibrils are not associated sufficiently with the surface. Long drying times (hours) will result in very stiff collagen fibrils

that appear to adhere to one another. Cells on stiff collagen fibrils respond to this mechanical stimulus by increased spreading, higher rates of proliferation, and changes in gene expression. Visualization of the collagen fibrils is possible with phase microscopy.

4. *Cell fixation and staining for quantifying cellular GFP*: we typically examine transfected cells with constructs of GFP linked to a promoter region of interest. As a result, we are measuring soluble GFP that is present in the cytoplasm of the reporter cells; the GFP is not fused to another protein. Fixing these GFP-expressing cells with formaldehyde in PBS results in the attenuation of the GFP signal by >50%. To prevent GFP signal reduction during fixation, we found that the use of MTSB (10) and the MBS crosslinker resulted in the preservation of greater than 90% of the initial GFP fluorescence signal with no loss in cell morphology.
5. *Bleed-through of fluorescence from other fluorophores*: careful control experiments must be performed when developing protocols for the use of more than one dye in quantitative analysis. Control samples that contain each dye alone, then in combination, must be examined under the conditions that will be ultimately used for data collection, including lamp intensity, filter sets, integration time, and so on. The conditions described above were selected for unambiguous quantification of GFP expression levels.
6. *Thresholding*: potential caveats associated with automated microscopy include assigning the threshold intensity that will be applied to images to discriminate between cell area and background. If the staining at the cell periphery is very bright relative to background, a range of threshold values can be applied that do not significantly affect the data (6). However, under other circumstances, thresholding can be a source of inconsistency in datasets. Development of robust algorithms for choosing appropriate threshold values will be a challenge to be overcome.
7. *Quantifying GFP*: the use of a general cell stain like Texas Red maleimide to provide a cell “mask,” allows us to easily identify all cells and to quantify GFP even in those cells that do not express much GFP. In this way, we can quantify the difference between cells in conditions in which the associated promoter is very active, inactive, or of intermediate activity. It must be noted that we are describing a procedure for achieving only relative quantitative analysis; determining absolute concentration of a fluorophore by microscopy is by far a more challenging issue.
8. *Background determination using erosion*: erosion is a technique that can be used for determining the background fluorescence that should be subtracted from a cell image. It is particularly useful when the background varies widely across the field such that an average background value would not be appropriate for all cells in the field. A large standard deviation in the intensity of the eroded pixels can be the result of the presence debris or another cell, or an indication that the cell lies partially outside of the frame; the standard deviation thus can be a flag that precludes the use of that background determination.

References

1. Geiger, B., Bershadasky, A., Pankov, R., and Yamada, K. M. (2001) Transmembrane extracellular matrix-cytoskeleton crosstalk. *Mol. Cell Biol.* **2**, 793–805.
2. Elliott, J. T., Jones, P. L., Woodward, J. T., Tona, A., and Plant, A. L. (2002) Morphology of smooth muscle cells on thin films of collagen. *Langmuir* **19**, 1506–1514.
3. Elliott, J. T., Langenbach, K. J., Tona, A., Jones, P. L., and Plant, A. L. (2005) Vascular smooth muscle cell response on thin films of collagen. *Matrix Biol.* **24**, 489–502.
4. Langenbach, K. J., Elliott, J. T., Tona, A., and Plant, A. L. (2005) Evaluating the correlation between fibroblast morphology and promoter activity on thin films of extracellular matrix proteins. *BMC-Biotechnology* (in press).
5. Elliott, et al. The effect of surface chemistry on the formation of thin films of native fibrillar collagen. (in preparation).
6. Elliott, J. T., Tona, A., and Plant, A. L. (2002) Comparison of reagents for shape analysis of fixed cells by automated fluorescence microscopy. *Cytometry* **52A**, 90–100.
7. Perlman, Z. E., Slack, M. D., Feng, Y., Mitchison, T. J., Wu, L. F., and Altschuler, S. J. (2004) Multidimensional drug profiling by automated microscopy. *Science* **306**(5699), 1194–1198.
8. Giuliano, K. A., Chen, Y. -T., and Taylor, D. L. (2004) High content screening with siRNA optimizes a cell biological approach to drug discovery: defining the role of p53 activation in the cellular response to anti-cancer drugs. *J. Biomol. Screen.* **9**, 557–567.

9. Jones, P. L., Crack, J., and Rabinovitch, M. (1997) Regulation of tenascin-C, a vascular smooth muscle cell survival factor that interacts with the $\alpha v \beta 3$ integrin to promote epidermal growth factor receptor phosphorylation and growth. *J. Cell Biol.* **139**, 279–293.
10. Safiejko-Mroczka, B. and Bell, P. B., Jr. (1996) Bifunctional protein cross-linking reagents improve labeling of cytoskeletal proteins for qualitative and quantitative fluorescence microscopy. *J. Histochem. Cytochem.* **44**, 641–656.
11. Wyszecki, G. and Stiles, W. S. (1967) *Color Science: Concepts and Methods, Quantitative Data and Formula*, Wiley, New York, NY.